Indian Geotechnical Journal, 33 (4), 2003

Nonlinear Time Domain Analysis of Single Piles by FEM

B.K. Maheshwari*, K.Z. Truman† and M.H. El Naggar‡

Introduction

Recent devastating earthquakes (e.g. Bhuj, 2001; Chi-Chi, 1999; Kocaeli, 1999; Kobe, 1995 and Northridge, 1994) have shown that the collapse of many buildings was due to the failure of the supporting pile foundations. Much of the research performed in the last three decades for dynamic analysis of pile foundations assumes linear behavior of the soil media. For example, Kaynia and Kausel (1982), Gazetas (1984) and Makris and Gazetas (1992) proposed linear analyses of single piles and pile groups in the frequency domain. Maheshwari and Watanabe (1998) used the equivalent linearization technique to include the material nonlinearity of the soil in the frequency domain. However, the equivalent linearization techniques were not suitable for the analysis of strong earthquakes as the level of shear strain in the soil media can be extremely high. The nonlinear conditions expected during earthquake loading can only be accurately modeled using time domain analyses.

Matlock et al. (1978) developed a unit load transfer curve approach, also known as p-y curves, for nonlinear analysis of piles in the time domain. Nogami and Konagai (1986 and 1988) developed a time domain analysis method for the axial and lateral response of single piles, respectively. They used the soil reactions proposed by Novak et al. (1978) that assumed a plane

* Postdoctoral Researcher, Dept. of Civil Eng., Washington Univ., St. Louis, MO 63130, USA. E-mail: balkrishna@hotmail.com

† Professor and Chairman, Dept. of Civil Eng., Washington Univ., St. Louis, MO 63130, USA

‡ Assoc. Prof., Dept. of Civil Eng., Univ. of Western Ontario, London, Ontario N6A 5B9, Canada

strain continuous elastic medium within the framework of the Winkler soil model. However, in these analyses, the nonlinear behavior of the soil media was not explicitly modeled. Strong excitation that causes severe nonlinearity warrants analysis in the time domain.

Nogami et al. (1992) accounted for material and geometrical nonlinearity in the analysis using discrete systems of mass, springs and dashpots. El Naggar and Novak (1995 and 1996) presented a nonlinear analysis for pile groups in the time domain using the Winkler hypothesis. However, it is difficult to properly represent damping and inertia effects of continuous, semi-infinite soil media using these simplifying models. Further, full coupling in the axial and lateral direction may not be considered. Inclusion of nonlinearity caused by the plasticity of the soil and the separation at the soil-pile interface requires that an analysis be performed in the time domain using the finite element approach..

Wu and Finn (1997) presented a quasi-3D method that used strain dependent soil properties and a tension cutoff. Bentley and El Naggar (2000) analyzed the kinematic response of single piles using the finite element approach. They used the Drucker-Prager soil model to account for the plasticity of soil but did not consider work hardening of the soil media. Cai et al. (2000) included the soil plasticity and work hardening of soil using a finite element technique in the time domain. However, they assumed fixed boundary conditions and neglected damping in the foundation subsystem. Moreover, the effects of soil nonlinearity on pile response were not examined.

Maheshwari et al. (2002) analyzed the effect of material nonlinearity on free field response and kinematic response of single piles using an advanced plasticity based soil model HiSS (Wathugala and Desai, 1993) in a finite element formulation. In this paper, this model is extended to account for gapping and the effects of geometrical nonlinearity on the pile's response. The effects of soil nonlinearity on the seismic response and impedance functions of piles are investigated. Though results presented in this paper are only for single piles, however the model and algorithm are already extended for pile groups as shown by Maheshwari et al. (2003).

Modeling Soil-Pile System

The soil-pile system is represented using full three-dimensional geometric models. However, taking advantage of symmetry and anti-symmetry (as shown in Fig.3a), only one fourth of the actual model was considered, thus improving efficiency of computation by many-folds and time required for computation using quarter model is less than (1/16) of that needed using full model. The finite element quarter model used for the soil-pile system is shown in Fig.1. The pile is fully embedded in the soil and is assumed to be

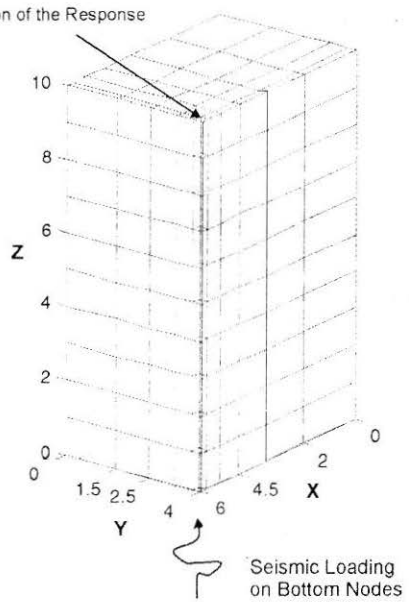

FIGURE 1 : 3-D Finite Element Quarter Model Used for the Soil-Pile System

bearing on the bedrock. The soil-pile system is idealized as an assemblage of eight-node hexahedral elements. Each node has three translational degrees of freedom along the coordinates X, Y and Z as shown in Fig.2a. The eight-node brick elements used in the model are suitable since the soil and pile responses are dominated by shear deformations rather than bending stresses. However, 20-node solid elements can be used for higher accuracy.

Kelvin elements (Fig.2b) are attached to the model side-walls in all

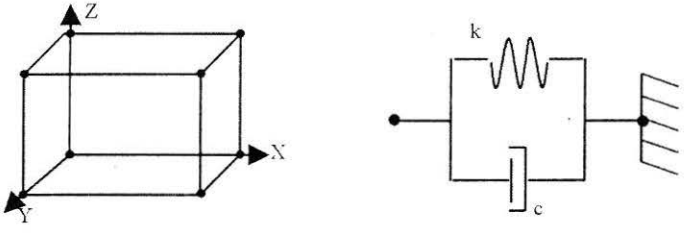

(A) 8-noded Block Element (B) 2-noded Boundary Element

FIGURE 2 : (a) Block Element Used for Soil and Pile (b) Boundary Element (Spring and Dashpot)

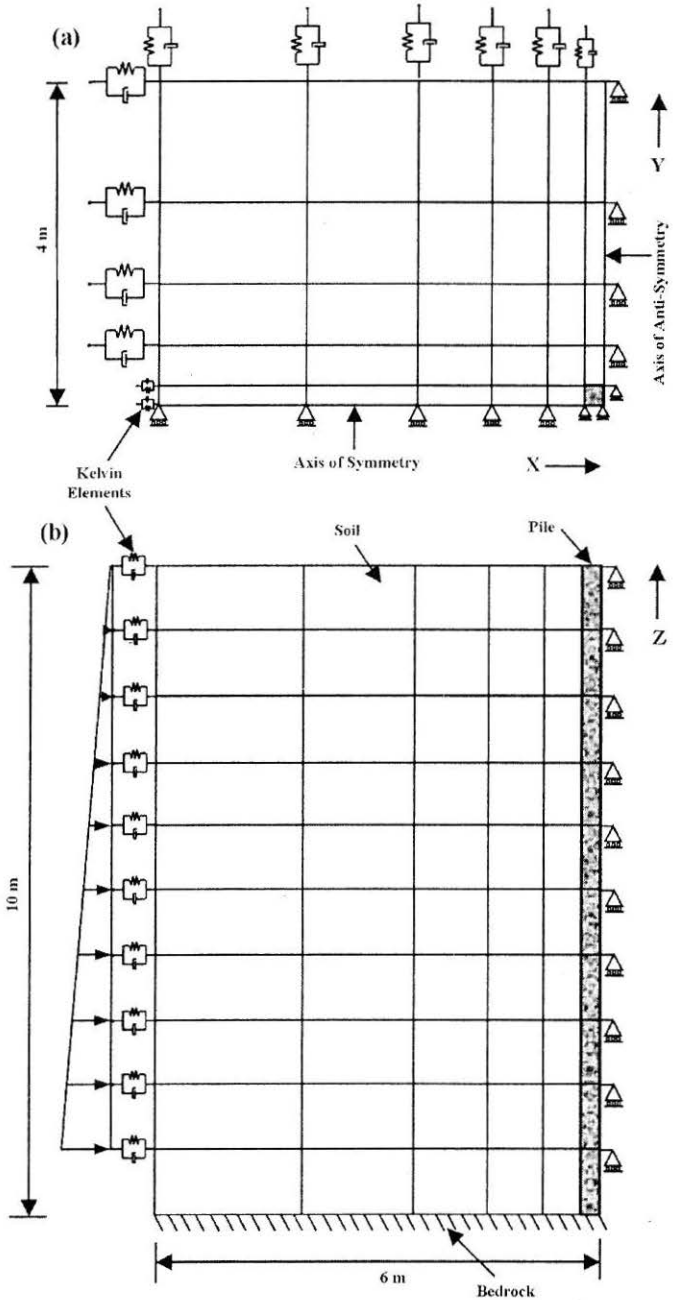

FIGURE 3 : Finite Element Mesh for Quarter Model showing Boundary Conditions: (a) Top Plan (b) Front Elevation with Initial Pressure Distribution

three directions in order to provide proper boundary conditions and to allow for wave propagation. Figures 3a and 3b show the details of the finite element mesh in plan and elevation, respectively. The mesh is refined near the pile and the element size increases gradually as they move away from the pile. The size of the elements near the pile is kept less than one sixth of the wavelength that corresponds to the highest frequency of 20 Hz considered in the analysis (Kramer, 1996). The dimensions of the mesh for the quarter model are 6 m × 4 m in plan and 10 m high. The elements varied from 0.25 m to 2 m in the horizontal direction but are kept constant at 1m in the vertical direction to allow for an even distribution of vertically propagating SH waves. The mesh comprised 300 elements.

The separation between the soil and pile is considered by not allowing any tension to occur in the soil elements adjacent to the pile. Pile elements are assumed to be linear but they can also be nonlinear using an appropriate constitutive relation. For the nonlinear soil model (HiSS), the initial stress condition in the soil is governed by the confining pressure of the soil and is proportional to the depth (Fig.3b). The seismic excitation is assumed to act on the fixed base nodes and is assumed to consist of vertically propagating shear waves. Since the analysis is in the time domain, a complete three-dimensional excitation can also be considered.

Processes of Analysis

Governing equation and solution

The governing equation of motion at time $t+\Delta t$ is:

$$M\,{}^{t+\Delta t}\ddot{U}+C\,{}^{t+\Delta t}\dot{U}+K\,{}^{t+\Delta t}U = {}^{t+\Delta t}R \qquad (1)$$

where

- M = diagonal mass matrix (all masses are lumped at the nodal points);
- C = global damping matrix and includes the effects of both material damping and radiation damping (dashpots) along the boundary;
- K = symmetric stiffness matrix determined with full coupling in all three directions of motion and includes the stiffness of springs at the boundary nodes;
- U = relative nodal displacement at $t+\Delta t$;
- $\dot{U}$ = relative nodal velocity at $t+\Delta t$;
- $\ddot{U}$ = relative nodal acceleration at $t+\Delta t$; and
- ${}^{t+\Delta t}R$ = external load.

Employing the constant average acceleration method of integration (Bathe, 1982), Eqn.(1) is solved for displacement ${}^{t+\Delta t}U$. For the linear case, the analysis is performed incrementally. When the soil plasticity is considered, matrices K and C change after each time step and the modified Newton-Raphson iteration scheme is used for the solution.

Boundary conditions

To simulate radiation conditions, Maheshwari et al. (2001) used frequency independent viscous dampers However in the present study the Kelvin elements are used because these include springs to model the medium's stiffness and lead to a better performance compared to the standard viscous boundary (Wolf, 1985; Novak and Mitwally, 1988). The Kelvin elements allow the use of a much smaller mesh size than that needed when using viscous dampers. To evaluate the constants of the Kelvin elements used in the time domain analysis, a Fourier spectrum of the excitation time history is derived and the predominant frequency of loading is determined. The stiffness and damping constants of the Kelvin model are then evaluated based on the predominant frequency of loading. The constants of the Kelvin element's spring and dashpot in the two horizontal directions are calculated using the solution developed by Novak and Mitwally (1988) and are given by:

$$k_r^* = \frac{G}{r_0}\left[S_1(a_r, \nu_s, D) + iS_2(a_r, \nu_s, D)\right] \tag{2a}$$

where k_r^* = complex stiffness,

G = shear modulus of soil,

S_1 and S_2 = dimensionless parameters obtained from closed-form solutions,

D = material damping ratio,

ν_s = Poisson's ratio, and

i = imaginary unit = $\sqrt{-1}$.

Also, r_0 is the distance in plan from the center of the pile to the node where the Kelvin element is attached and a_r is the dimensionless frequency $(= r_0\omega/V_s)$, where ω is the angular frequency of excitation and V_s is the shear wave velocity of the soil. The real and imaginary parts of Eqn.(2a) represent the stiffness and damping, respectively, i.e.

$$k_r = \frac{GS_1}{r_0} \quad \text{and} \quad c_r = \frac{GS_2}{\omega r_0} \tag{2b}$$

For the static loading case, the damping term vanishes and the element reduces to a spring only. Similarly, the constants for the vertical direction are given by Novak et al. (1978):

$$k_w^* = \frac{G}{r_0}\left[S_{w1}(a_r, D) + iS_{w2}(a_r, D)\right] \tag{3a}$$

where the subscript w is used to represent the vertical direction and the other parameters are the same as in Eqn.(2a).

Stiffness and damping for the vertical direction are determined in a similar fashion as mentioned in Eqn.(2b) i.e.

$$k_w = \frac{GS_{w1}}{r_0} \quad \text{and} \quad c_w = \frac{GS_{w2}}{\omega r_0} \tag{3b}$$

To determine the stiffness and damping of the Kelvin elements, the constants given by Eqns.(2b) and (3b) are multiplied by the area of the element face (normal to the direction of loading). It should be noted that for the vertical direction the dimensionless parameters S_{w1} and S_{w2} are independent of Poisson's ratio and for the static case both the spring and dashpot terms vanish. Thus, for the low frequency range, the spring and dashpot constants are adjusted to match more rigorous solutions by choosing a minimum cutoff frequency (a_r = 0.3) below which the stiffness is taken to be constant (= 2) and the damping is taken to be linear.

The boundary conditions at the axes of symmetry and anti-symmetry are shown in Fig.3. The nodes on the axis of symmetry are free to move in the vertical direction and along the direction of the axis of symmetry, and are fixed in the perpendicular horizontal direction. The nodes on the axis of anti-symmetry are constrained in both the vertical direction and the direction of this axis and are free to move in the perpendicular horizontal direction. All the nodes along the base are fixed in all three directions (Fig.3b). Two loading conditions were considered in the analysis. For seismic response external force is due to vertically propagating shear waves applied at fixed nodes. For determination of dynamic stiffness harmonic excitation is applied at the pile head.

System damping

To adequately represent damping in the system, both radiation and material damping are considered in the analysis. The damping matrix C consists of two parts; radiation damping, C_r, and material damping, C_m, i.e.

$$C = C_r + C_m \tag{4a}$$

The matrix of radiation damping, C_r is diagonal and has non-zero terms only at the nodes (on the boundary) where the Kelvin elements are attached. The matrix of material damping, C_m is taken to be proportional to stiffness (Guin and Banerjee, 1998) and is given by:

$$C_m = \alpha K \tag{4b}$$

where $$\alpha = 2D/\omega_0 \tag{4b}$$

where D is the material damping ratio and ω_0 is the predominant circular frequency of loading. Additional hysteretic damping may develop due to the nonlinearity. However, dissipation of seismic energy through inelastic deformation tends to overshadow the dissipation of the energy through hysteretic damping as shown by Anderson (1989) and is therefore neglected.

Nonlinear soil model

To introduce the effect of plasticity, the δ_0^* version of the nonlinear soil model HiSS (hierarchical single surface) proposed by Wathugala and Desai (1993) is used. Both plasticity and work hardening of the soil are considered in the model. The model is based on an incremental stress-strain relationship and assumes associative plasticity. Further, for the δ_0^* version of HiSS model, the constitutive relationship for nonvirgin loading (i.e. loading or unloading) is assumed elastic. The δ_0 version denotes the basic model for initially isotropic material, hardening isotropically with associative plasticity that involves zero deviation from normality δ_0 of the increment of plastic strain to the yield surface F. Superscript * is used to denote a modified series of models specially developed to capture the behavior of cohesive soils. The material parameters (of the model) for a marine clay found near Sabine Pass, Texas, were determined from laboratory tests (Katti, 1991) and verified with available data from field tests in "Pile Segment (1986)".

A simplified formulation used in virgin loading in HiSS is described here; a detailed formulation can be found in Wathugala and Desai (1993). In this model, a material parameter β is used to define the shape of the yield surface in the octahedral plane. Assuming $\beta = 0$ as was the case for Sabine Clay, the dimensionless yield surface F can be simplified as:

$$F = \left(\frac{J_{2D}}{p_a^2}\right) + \alpha_{ps}\left(\frac{J_1}{p_a}\right)^{\eta} - \gamma\left(\frac{J_1}{p_a}\right)^2 = 0 \tag{5a}$$

where J_1 = first invariant of the stress tensor σ_{ij};

J_{2D} = second invariant of the deviatoric stress tensor;

p_a = atmospheric pressure;

γ and η = material parameters that influence the shape of F in $J_1 - \sqrt{J_{2D}}$ space;

Parameter η is related to the phase change point defined as the point where material changes from contractive to dilative behavior (Fig.4).

In Eqn.(5a), α_{ps} is the hardening function defined in terms of plastic strain trajectory ξ_v, as:

$$\alpha_{ps} = h_1 / \xi_v^{h_2} \tag{5b}$$

where h_1 and h_2 = material parameters, and

ξ_v = trajectory of the volumetric plastic strain.

Typical yield surfaces in $J_1 - \sqrt{J_{2D}}$ space for this model are shown in Fig.4.

Separation at the pile-soil interface

Separation at the soil-pile interface, particularly near the pile heads, may occur during strong ground motions or loading from the pile head leading to high inertial forces. The pile-soil interface forces in the top layers of soil are high and the resisting forces due to the confining pressure are

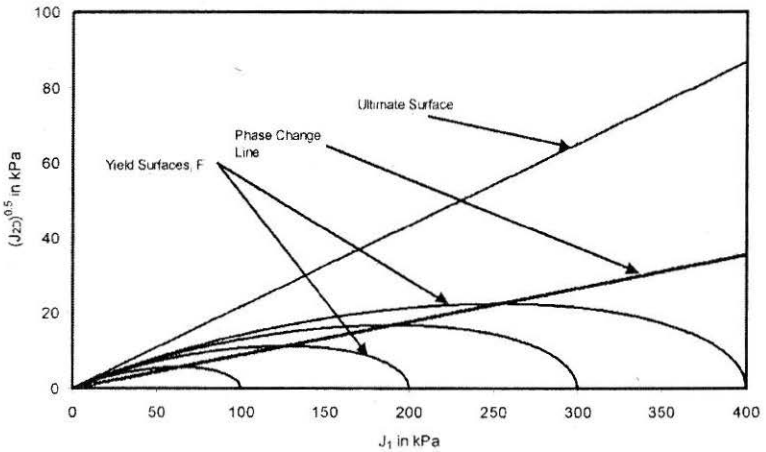

FIGURE 4 : Shape of Yield Surfaces

low. Thus, separation starts from the top layers and heads downward to a larger depth. In the present analysis, separation (or gapping) is approximately taken into account by allowing limited tension (until naturally existing compressive confining pressure in the soil is exhausted) in the soil elements. To include the effect of separation in the algorithm, it is modified as follows.

For a 3D model loaded in one direction, it is assumed that separation occurs in the direction of loading only and the soil and pile are still in contact in the other horizontal direction. Friction at the pile-soil interface is neglected. At every time step and at every iteration within a time step, the normal stresses in the soil elements (in the direction of loading) are checked for each Gaussian point against the confining pressure at that depth. Separation is assumed if the tensile normal stress exceeds the confining pressure. During separation, the constitutive stiffness matrix of the soil is modified by sharply reducing the stiffness of elements corresponding to the direction of loading.

For the elastic case, the constitutive stiffness matrix reduces to that corresponding to a plane stress case. When the stresses in the soil elements during load reversal are again within limits, the full value of the constitutive stiffness matrix is restored. It is noted that when separation is considered in the analysis even an elastic soil model requires an iterative scheme to check the convergence at every time step. Therefore, the computation time increases significantly.

Seismic excitation

The control point for seismic loading is assumed at the bedrock and thus the external force in the equation of motion is found by (Clough nd Penzien, 1993):

$$^{t+\Delta t}R = -MP_F\,{}^{t+\Delta t}\ddot{V}_b \qquad (6)$$

where P_F = pseudostatic response influence coefficient vector, and

$\ddot{V}_b$ = bedrock acceleration at time $t+\Delta t$, due to vertically propagating shear waves.

Impedance Functions of the Soil-Pile System

The impedance function (or dynamic stiffness), K_c, includes the static stiffness of the system as well as the effects of inertia and damping. In the frequency domain, this is a complex quantity and can be determined at a particular frequency ω by:

$$K_c = k_{st} - \omega^2 M + i\omega C \tag{7a}$$

where k_{st} is the static (true) stiffness of the system and M is its mass.

Alternatively, the complex dynamic stiffness K_c, can be evaluated in the frequency domain by applying a real load with a given amplitude, P_0, at the pile head and noting the complex response amplitude, U_c, of the pile head, i.e.

$$K_c = P_0/U_c \tag{7b}$$

The dynamic stiffness of piles is a function of the loading level and frequency. In the current time domain analysis, the stiffness of the piles is evaluated as follows. For the quarter model, a harmonic lateral load of amplitude P_0 equal to 12.5 kN is applied at the pile head and the resulting displacement at the same point is noted for different frequencies of excitation. This value of load (i.e. 50 kN for a full pile) is selected to ensure that soil yielding occurs and the response becomes nonlinear. Also, this level of loading was found to cause separation at the pile-soil interface. After the response stabilizes (i.e. becomes steady state), the peak amplitude of the response, U_0, and its time lag, t_l, with respect to the applied force amplitude are noted from the time history of the resulting displacement at the pile head. With these observations, the phase lag θ (in radians) and complex dynamic stiffness of the soil-pile system can be found as follows:

$$\theta = \omega t_l = 2\pi f t_l \tag{7c}$$

$$K_c = (P_0/U_0)e^{i\theta} \tag{7d}$$

where f is the frequency of excitation in Hz.

Separating the dynamic stiffness, given by Eqn.(7d), into real and imaginary parts, the pile spring constant (including effect of inertia) and damping constant can be determined.

Computerization

A FORTRAN program (3dNDPILE) was developed to perform the analysis. Finite element programming strategies suggested by Zienkiewicz (1977), Bathe (1982) and Wathugala (1990) have been incorporated in the development of the program. For the nonlinear analysis, three criteria, namely the displacement criteria, the out-of-balance load criteria and the internal energy criteria, are used simultaneously to check the convergence of the

iteration (Bathe, 1982). To save space used to store the matrices, a skyline storage scheme (Zienkiewicz, 1977) is adopted. Special procedures (Wathugala, 1990) are used to ensure the robustness of the HiSS iterative solution. These special procedures are further enhanced to deal with the case when the plasticity parameter (λ) becomes negative. The plasticity parameter is a constant of proportionality and is used to define the flow rule of plasticity, (Chen and Baladi, 1985) as follows:

$$d\varepsilon_{ij}^{p} = \lambda \frac{\partial F}{\partial \sigma_{ij}} \tag{8}$$

The left hand side of Eqn.(8) defines the plastic strain increment tensor. Convergence of the dimensionless yield surface (F) is assumed when its absolute value becomes fairly small, i.e. when ABS(F) < 10^{-10}. For harmonic excitations, the step size is assumed to be (T/20) where T is the period. The algorithm developed is quite efficient and economical and computation time is reduced due to the use of the quarter model, therefore, nonlinear analyses can be performed on a modern P.C. and a workstation is not required for the computation. The analyses reported herein are performed on a Pentium P.C. (with Windows XP OS, 664 MHz speed and 768 Mb RAM). Computational time for the static analysis is less than 30 seconds even for the nonlinear analysis. A dynamic elastic analysis for a 30 s earthquake (with 0.02 s time interval) requires about five minutes and the nonlinear analysis requires less than two hours.

Data Used in Computation

Table 1, shows the data used in the analyses. For the transient motion, an acceleration time history for the El Centro Earthquake (Chopra, 1995) has been used (Fig.5a; shown only for the first 20 s). Figure 5b shows a smoothed Fourier spectrum for this time history. The response (acceleration) shown in all results is that at the pile head.

Verification of the Model and Algorithm

The proposed finite element model and developed algorithm need to be verified. This is performed using elastic and elasto-plastic analyses and the results are compared with those found in the literature. The verification is carried out for static as well as dynamic loading.

Verification for static loading

Figure 6 shows a schematic of the problem considered for static verification which involves the lateral loading of an end-bearing pile from

TABLE 1 : Data Used in Computation

Properties of Soil (Sabine clay) Desai and Wathugala (1993)	
Young's modulus (E_s)	11.777 MPa
Mass density (ρ_s)	1610 kg/m^3
Poisson's ratio (ν_s)	0.42
Material damping ratio (D)	0.05
Parameters of HiSS model:	
γ	0.047
η	2.4
h_1	0.0034
h_2	0.78
Properties of Pile (Concrete)	
Young's modulus (E_p)	25000 MPa
Mass density (ρ_p)	2400 kg/m^3
Poisson's ratio (ν_p)	0.25
Length (L)	10 m
Cross section (square), side (d)	0.5 m
Seismic Loading	
Harmonic	sinusoidal wave
Amplitude (Acceleration)	Unit (1 m/s^2)
Frequency	Varying
Transient	El Centro Earthquake 1940 (N-S component)
PGA	0.32g
Predominant frequency	1.83 Hz
Loading from Pile Head	
Harmonic: sinusoidal wave	
Amplitude (Force)	12.5 kN
Frequency	Varying

the top. The geometry and properties of the soil-pile system, which are the same as those used by Bentley and El Naggar (2000), are also shown in Fig.6.

Horizontal deflections of the pile head are computed for different amplitudes of applied load for the elastic and plastic cases. The results are shown in Figs.7a and 7b for the elastic and plastic cases, respectively. These results are compared with the results presented in Bentley and El Naggar (2000) (including those produced by other authors). Bentley and El Naggar (2000) have shown results using three different meshes and concluded that

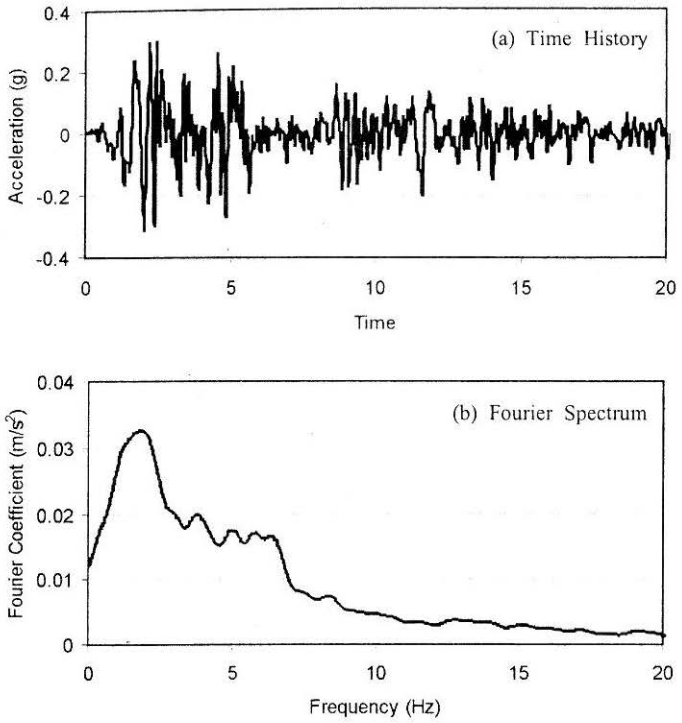

FIGURE 5 : Input Bedrock Motion for Transient Analysis, El Centro Earthquake (N-S Component)

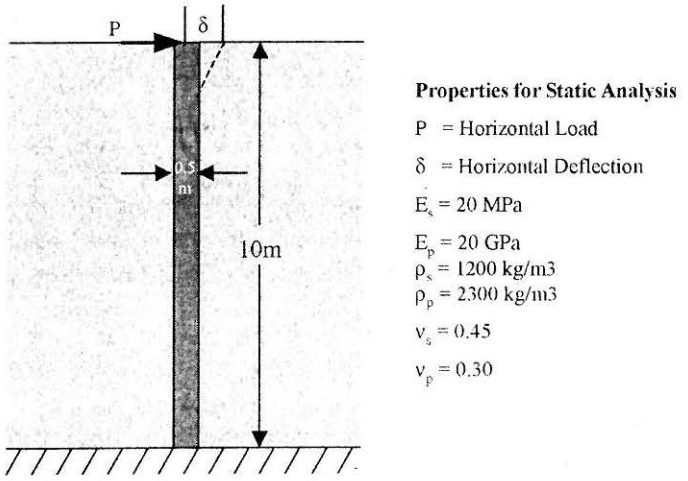

FIGURE 6 : Soil-Pile System for Static Loading

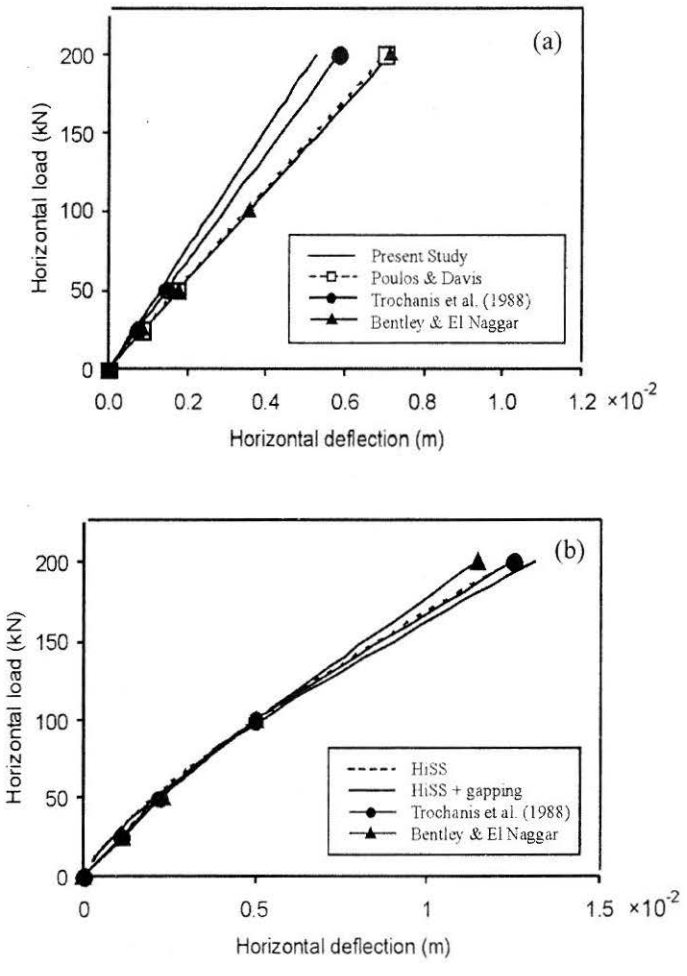

FIGURE 7 : Verification for Static Loading (a) Elastic (b) Plastic

finest mesh (i.e. mesh # 3) gives the best results, therefore for verification, only the mesh # 3 is used here. It can be seen that for the elastic case (Fig.7a), the results are in good agreement with those of a FEA study by Trochanis et al. (1988) who considered a square pile similar to the current case, but the deflections evaluated by the present model are slightly less than those for Bentley and El Naggar (mesh # 3), and Poulos and Davis (1980) who considered a circular pile cross-section. For the plastic case, analyses with and without gapping were performed and the results are presented in Fig.7b and compared with the response obtained by Trochanis et al. (1988), and Bentley and El Naggar (2000) for elasto-plastic soil with gapping. It can be seen that the results obtained from all approaches agree well, even though

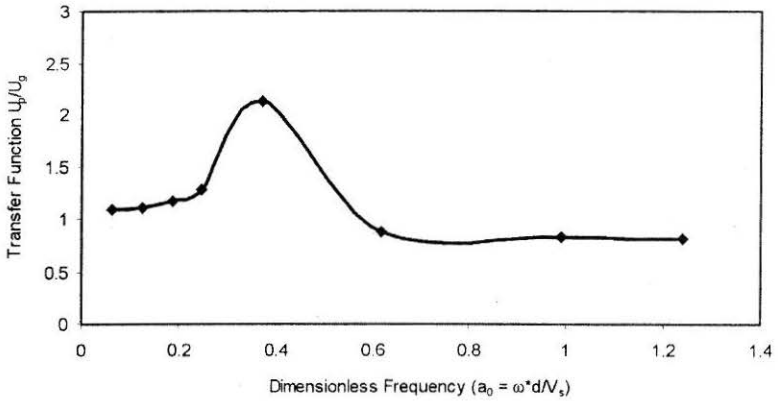

FIGURE 8 : Verification for Dynamic Loading

different plasticity models were used (HiSS here and Drucker-Prager in other studies). This verifies the model for static loading. It can also be observed from Fig.7b that when gapping is allowed for a HiSS soil model, the increase in response due to gapping is not significant. It appears that the effect of plasticity overshadows the effect of separation.

Verification for dynamic loading

The response time histories for the free field (assuming no pile) and the pile head are derived for harmonic excitations with different frequencies for the elastic soil model. The amplitude of the steady state free field response, U_g, and the pile head response, U_p, are noted from the response time history and the transfer function, U_p/U_g, are derived for different frequencies and presented in Fig.8 in terms of the dimensionless frequency, $a_0 = \omega d/V_s$.

Figure 8 shows that the value of the transfer function is slightly more than unity for $a_0 < 0.3$ and less than unity at higher frequencies. The transfer function displays a peak value slightly greater than two at $a_0 \approx 0.4$ (near the natural frequency of the soil-pile system). Kaynia and Kausel (1982) suggest that the value of the transfer function for a single pile is slightly more than unity for lower and moderate values of a_0 and decreases significantly at higher frequencies. This verifies the model for dynamic loading. The free field response evaluated using the model for transient excitation compared well with that obtained using SHAKE91 (Maheshwari et al., 2002).

Effects of Soil Nonlinearity on Pile Behavior

The effects of material and geometrical nonlinearity on the response of

the soil-pile system are investigated. The effects of soil plasticity on the seismic response are investigated first followed by examining the effects of soil nonlinearity on the dynamic stiffness of the system. In these two cases, gapping at the soil-pile interface is neglected and a perfect bond is assumed. The effects of separation on the dynamic stiffness are then investigated for both the elastic and HiSS soil models. This enables evaluating the relative importance of soil plasticity and gapping at the soil-pile interface on the behavior of the soil-pile system.

Effects of Soil Plasticity on Pile Seismic Response

The effects of soil plasticity (including work hardening) on the seismic response of a soil-pile system are observed. The linear and nonlinear responses of the pile head are evaluated for harmonic as well as transient excitation. For harmonic excitation, the effects of soil plasticity and the frequency of excitation on the pile response are investigated.

Analysis for harmonic excitations

The pile head response is obtained for harmonic excitations with different frequencies for the linear and nonlinear cases. The results are presented in Fig.9a in terms of the amplitude of pile head motion (U_p) normalized by the amplitude of the input bedrock motion (U_0). Figure 9a shows that the effect of soil nonlinearity on the pile head response is noticeable at low and moderate frequencies ($a_0 < 0.6$) but is insignificant at higher frequencies. At low frequencies ($0.15 < a_0 < 0.5$) the effect of nonlinearity increases the normalized response as much as 40% emphasizing the importance of nonlinear analysis.

The kinematic interaction factors or transfer functions (i.e. ratio of pile head response to the elastic free field response) are derived at discrete frequencies of excitation and are shown in Fig.9b. It can be seen that at low and moderate frequencies of excitation ($a_0 < 0.6$), the nonlinear interaction factor is significantly higher than the linear one but at higher frequencies there is little difference between the two.

Analysis for transient motion

Figure 10a shows the linear and nonlinear pile head responses due to the El Centro Earthquake loading (for clarity, only the initial 10 seconds are shown). It is observed that although the maximum acceleration amplitudes for elastic and plastic cases are almost the same, most of the other peaks are high for the plastic case. Bentley and El Naggar (2000) made a similar observation. The peak responses for the elastic and HiSS case are approximately 0.72g and 0.70g, respectively.

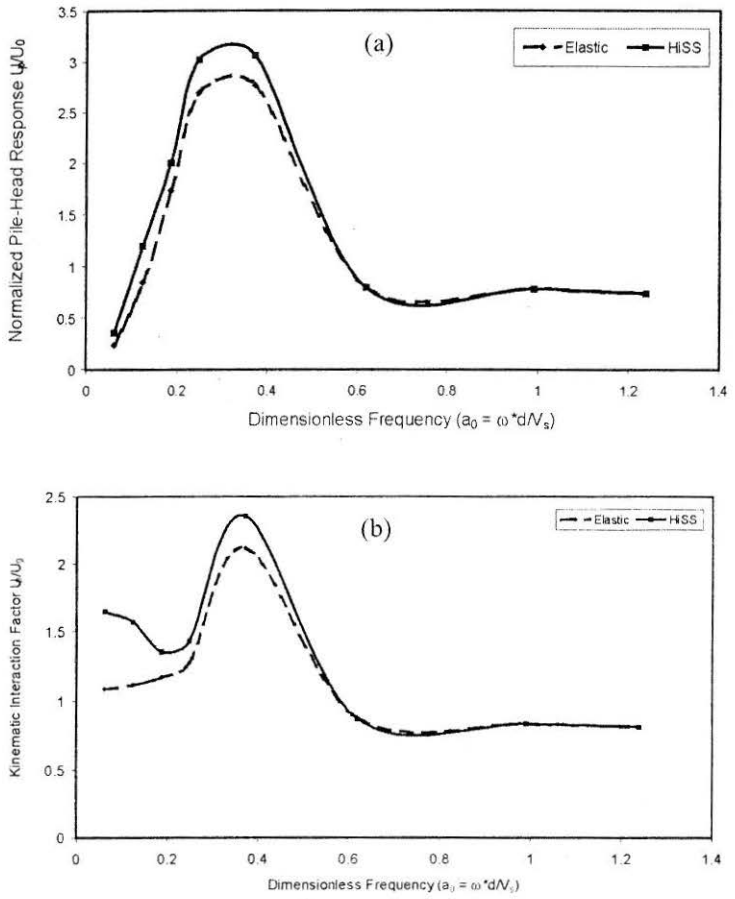

FIGURE 9 : Effect of Nonlinearity on (a) Pile Head Response at Different Frequencies; (b) Kinematic Interaction Factor

A smoothed Fourier spectrum of the pile head response is shown in Fig.10b. It is noted that the difference between the linear and nonlinear responses is noticeable and the Fourier amplitudes of the HiSS soil model are higher than that of the elastic soil model. The peaks for both models occur near 3.9 Hz (the second natural frequency of the soil-pile system). At higher frequencies (greater than 6 Hz), there is hardly any difference between the linear and nonlinear responses. However, the contributions to the structural response at these high frequencies are minimal.

Effects of Material Nonlinearity on Impedance Functions

The dynamic stiffness (or impedance functions) of the soil-pile system

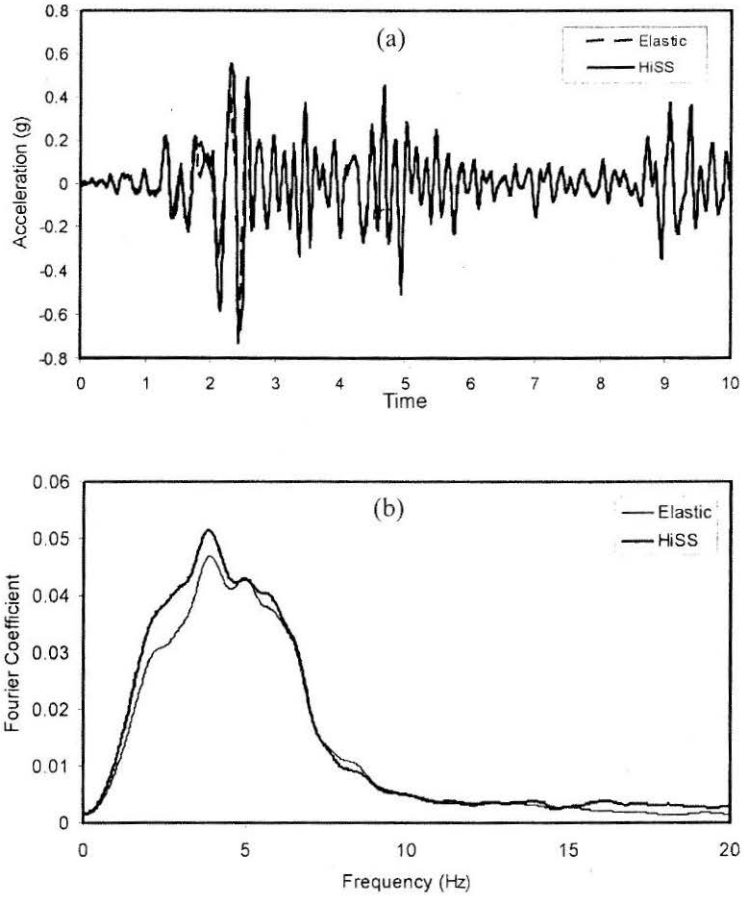

FIGURE 10 : Pile Head Response due to El Centro Earthquake (a) Linear and Nonlinear; (b) Comparison of Fourier Spectrum

must be known when evaluating the dynamic response of a structure supported by a pile foundation. During strong excitations, this stiffness is affected by the nonlinear soil behavior.

In the present study, the complex dynamic stiffness (K_c) is found using Eqn.(7d), and can be written as:

$$K_c = k + ik' \tag{9}$$

where the real part, $k = k_{st} - \omega^2 M$ represents the stiffness (including the effect of inertia) and the imaginary part, $k' = \omega C$ represents the damping. The dynamic stiffness of the system is evaluated using the linear (elastic)

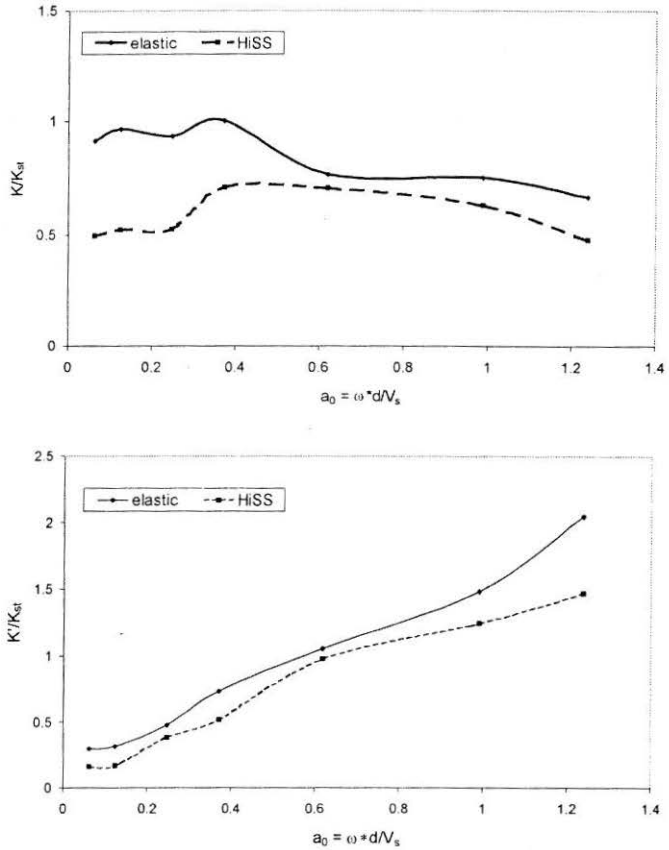

FIGURE 11 : Comparison of Linear and Nonlinear Dynamic Stiffness of the Soil-Pile System: (a) Real Part (b) Imaginary Part

and nonlinear (HiSS) soil models for different excitation frequencies. The results are presented in a dimensionless form. Figures 11a and 11b show the effects of soil nonlinearity on stiffness and damping, respectively. The dynamic stiffness is normalized with respect to the static stiffness of a single pile (k_{st}). Figure 11a shows that the normalized elastic stiffness of a single pile remains near unity at low frequencies, as has been observed by Kaynia and Kausel (1982).

Figure 11 shows that the soil nonlinearity reduces both stiffness and damping. However, its effect is more significant on the stiffness than it is on damping. The effect of the soil plasticity is to reduce the stiffness (Fig.11a) for all frequencies, but the effect is more significant at low frequencies ($a_0 < 0.4$). In this frequency range, the soil nonlinearity reduced the normalized stiffness to approximately one half of its elastic value. The effect

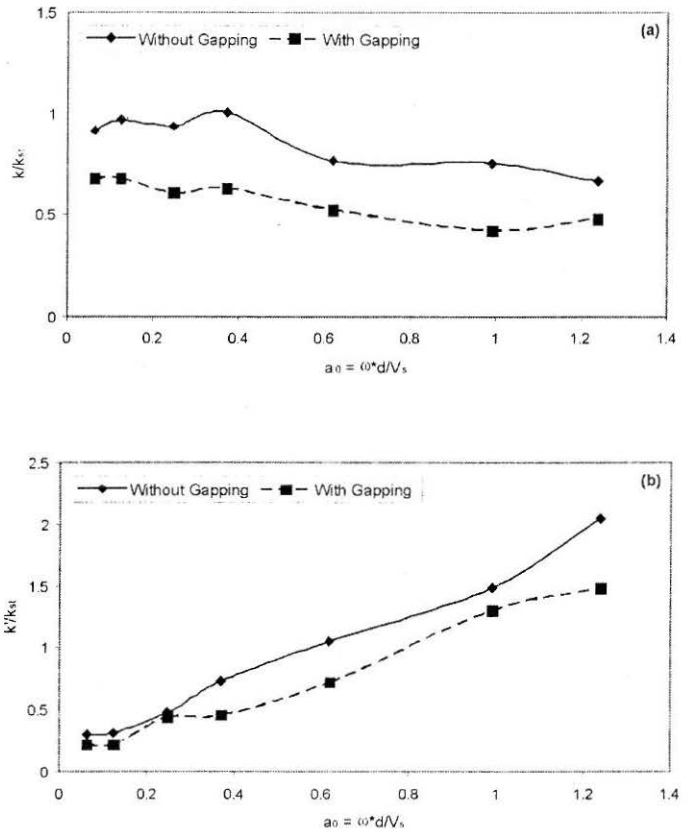

FIGURE 12 : Effect of Gapping on the Elastic Dynamic Stiffness of the Soil-Pile System: (a) Real Part (b) Imaginary Part

of soil nonlinearity on damping (Fig.11b) is less at low and moderate frequencies but greater at higher frequencies. For the nonlinear case, the damping increases almost linearly with frequency. Nogami and Konagai (1987) and Nogami et al. (1992) made similar observations using a Winkler soil model.

Effects of Geometrical Nonlinearity on Impedance Functions

For a soil-pile system, the possibility of separation between a pile and the soil is higher in the case of loading applied at the pile head (due to inertial effects) compared to the case of seismic loading through the soil. Therefore, the effects of separation are investigated only for the dynamic stiffness.

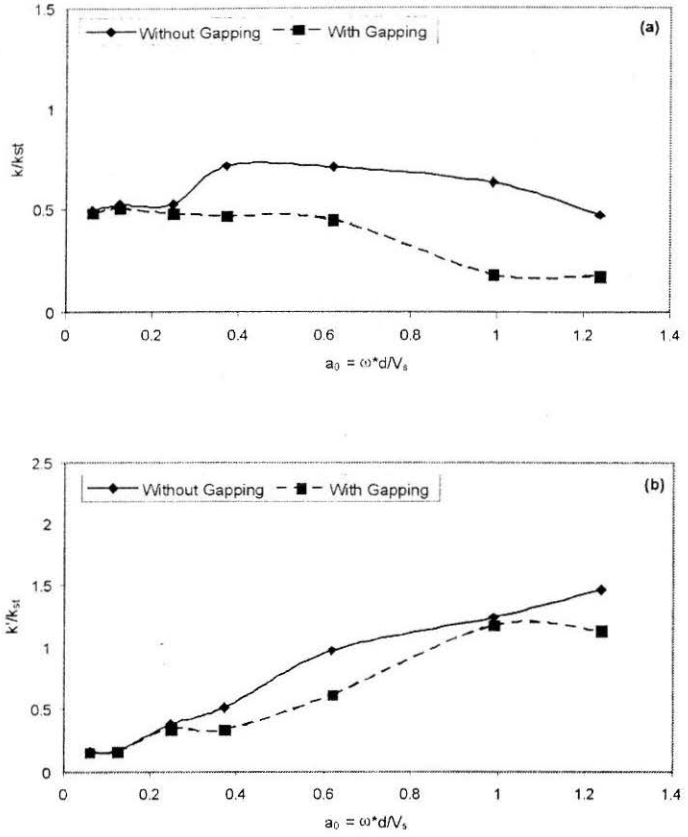

FIGURE 13 : Effect of Gapping on the Plastic Dynamic Stiffness of the Soil-Pile System: (a) Real Part (b) Imaginary Part

Elastic soil model

Figure 12 shows the effect of separation on the real and imaginary parts of the dynamic stiffness for the elastic soil model. Figure 12a shows that gapping significantly reduces the real part (stiffness) at all frequencies due to the lack of soil support along the pile segment where gapping occurs. Figure 12b shows that the effect of gapping on damping is not significant at low frequencies ($a_0 < 0.3$) but is considerable at high frequencies. This is because at higher frequencies radiation damping ceases to occur as there is no wave propagation along the gap.

Plastic soil model

Figure 13 shows the effect of gapping on the stiffness of the pile-soil system for the case of the plastic soil model. It is noted from Fig.13a that

the effect of gapping on the real part is not significant at low frequencies ($a_0 < 0.3$), unlike the case of the elastic soil. A similar observation is made for the static loading (Fig.7b). Trochanis et al. (1988) also conclude that when soil plasticity is considered in the case of static loading on piles, the nonlinear response is almost entirely due to soil plasticity and pile-soil separation does not result in additional nonlinearity. However, at higher frequencies the effect of gapping is more significant compared to the elastic soil model.

Figure 13b shows that gapping results in a decrease in the damping as wave propagation ceases along the gapping zone, especially in the high frequency range where the radiation damping represents a major portion of the total damping. The overall effect of gapping on damping is similar to that observed in the case of the elastic soil model.

Conclusions

The effects of material and geometrical nonlinearity on the behavior of single piles are investigated. A three-dimensional finite element dynamic technique in conjunction with the HiSS soil model is used. Analyses are performed for seismic excitations as well as for inertial loading. The linear and nonlinear pile responses are calculated. The following conclusions are drawn:

1. The effect of soil nonlinearity on the seismic response is significant at low and moderate frequencies that represent the range of interest for seismic loading. However its effect was insignificant at higher frequencies. For transient excitation, Fourier spectra further validate this observation.

2. The soil plasticity reduces both the real and imaginary parts of the dynamic stiffness but its effect on the real part is more pronounced, particularly at low frequencies.

3. For the elastic soil model, the effect of gapping on the pile stiffness was significant at all frequencies. However, for the plastic soil model, its effect is insignificant at low frequencies and considerable at high frequencies. It appears that at low frequencies plasticity overshadows the effect of gapping while at higher frequencies the effect of separation prevails due to an increase in inertial forces.

In general, nonlinearity significantly affects both dynamic stiffness and seismic response of a soil-pile system and its effect is much dependent on the frequency of excitation. Therefore, analyses presented may have an important bearing in the practical design of pile foundations.

Acknowledgement

The research presented here was partially supported by the Mid-America Earthquake Center under National Science Foundation Grant EEC-9701785 and the US Army Corps of Engineers. This support is gratefully acknowledged.

References

ANDERSON, J.C. (1989) : *Dynamic Response of Buildings*, the Seismic Design Handbook (edited by Naeim, F.), Van Nostrand Reinhold, New York, pp.113-118.

BATHE, K.J. (1982) : *Finite Element Procedures in Engineering Analysis*, Prentice-Hall, Inc., Englewood Cliffs, New Jersey.

BENTLEY, K.J. and El NAGGAR, M.H. (2000) : "Numerical Analysis of Kinematic Response of Single Piles", *Canadian Geotechnical Journal*, Vol.37, pp.1368-1382.

CAI, Y.X., GOULD, P.L. and DESAI, C.S. (2000) : "Nonlinear Analysis of 3D Seismic Interaction of Soil-Pile-Structure System and Application", *Engineering Structures*, Vol.22, No.2, pp.191-199.

CHEN, W.F. and BALADI, G.Y. (1985) : *Soil Plasticity: Theory and Implementation*, Elsevier, Amsterdam.

CHOPRA, A.K. (1995) : *Dynamics of Structures*, Prentice Hall, Inc., Upper Saddle River, New Jersey.

CLOUGH, R.W. and PENZIEN, J. (1993) : *Dynamics of Structures*, McGraw-Hill, Inc., Singapore.

DESAI, C.S. and WATHUGALA, G.W. (1993) : "Constitutive Model for Cyclic Behavior of Clays. II: Applications", *Journal of Geotechnical Engineering*, ASCE, Vol.119, No.4, pp.730-748.

El NAGGAR, M.H. and NOVAK M. (1995) : "Nonlinear Lateral Interaction in Pile Dynamics", *Soil Dynamics and Earthquake Engineering*, Vol.14, pp.141-157.

El NAGGAR, M.H. and NOVAK, M. (1996) : "Nonlinear Analysis for Dynamic Lateral Pile Response", Soil Dynamics and Earthquake Engineering, Vol.15, pp.233-244.

GAZETAS, G. (1984) : "Seismic Response of End-Bearing Single Piles", *Soil Dynamics and Earthquake Engineering*, Vol.3, No.2, pp.82-93.

GUIN, J. and BANERJEE, P.K. (1998) : "Coupled Soil-Pile-Structure Interaction Analysis under Seismic Excitation", *Journal of Structural Engineering*, ASCE, Vol.124, No.4, pp.434-444.

KATTI, D.R. (1991) : "Constitutive Modeling and Testing of Saturated Marine Clay", *PhD Dissertation*, Dept. of Civil Eng. and Eng. Mechanics, Univ. of Arizona, Tucson, Arizona.

KAYNIA, A.M. and KAUSEL, E. (1982) : "Dynamic Behavior of Pile Groups", *Proceedings of 2nd International Conference on Numerical Methods in Offshore Piling*, Austin, Texas, pp.509-532.

KRAMER, S.L. (1996) : *Geotechnical Earthquake Engineering*, Prentice Hall, Inc., Upper Saddle River, New Jersey.

MAHESHWARI B.K. and WATANABE H. (1998) : "Nonlinear Seismic Analysis of Pile Foundation",*Proceedings of 11th European Conference on Earthquake Engineering*, Paris, Paper No.283.

MAHESHWARI B.K., TRUMAN K.Z. and GOULD P.L. (2001) : "Application of Nonlinear Constitutive Model of Soil in Dynamic Soil-Pile Interaction using Finite Element Technique", *Proceedings of 2nd International Conference on Theoretical, Applied, Computational and Experimental Mechanics*, IIT Kharagpur, India.

MAHESHWARI, B.K., TRUMAN, K.Z., GOULD, P.L. and El NAGGAR, M.H. (2002) : *Three-Dimensional Nonlinear Seismic Analysis of Single Piles using FEM: Effects of Plasticity of Soil*, In review for International Journal of Geomechanics.

MAHESHWARI, B.K., TRUMAN, K.Z., El NAGGAR, M.H. and GOULD, P.L. (2003) : "3D FEM Nonlinear Dynamic Analysis of Pile Groups for Lateral Transient and Seismic Excitations", *Accepted for publication in Canadian Geotechnical Journal.*

MAKRIS, N. and GAZETAS, G. (1992) : "Dynamic Pile-Soil-Pile Interaction. Part II: Lateral and Seismic Response", *International Journal of Earthquake Engineering and Structural Dynamics*, Vol.21, pp.145-162.

MATLOCK, H., FOO, S.H.C. and BRYANT, L.M. (1978) : "Simulation of Lateral Pile Behavior under Earthquake Motion", *Proceedings of ASCE Specialty Conf. on Earthquake Engineering and Soil Dynamics*, Pasadena, California, pp.600-619.

NOGAMI, T. and KONAGAI, K. (1986) : "Time Domain Axial Response of Dynamically Loaded Single Piles", *Journal of Engineering Mechanics*, ASCE, Vol.112, No.11, pp.1241-1252.

NOGAMI, T. and KONAGAI, K. (1987) : "Dynamic Response of Vertically Loaded Nonlinear Pile Foundations", *Journal of Geotechnical Engineering*, ASCE, Vol.113, No.2, pp.147-160.

NOGAMI, T. and KONAGAI, K. (1988) : "Time Domain Flexural Response of Dynamically Loaded Single Piles", *Journal of Engineering Mechanics*, ASCE, Vol.114, No.9, pp.1512-1525.

NOGAMI, T., OTANI, J., KONAGAI, K. and CHEN, H.L. (1992) : "Nonlinear Soil-Pile Interaction Model for Dynamic Lateral Motion", *Journal of Geotechnical Engineering*, ASCE, Vol.118, No.1, pp.89-106.

NOVAK, M., NOGAMI, T. and ABOUL-ELLA, F. (1978) : "Dynamic Soil Reaction for Plane Strain Case", Technical Note, *Journal of Engineering Mechanics*, ASCE, Vol.104, No.4, pp.953-956.

NOVAK, M. and MITWALLY, H. (1988) : "Transmitting Boundary for Axisymmetrical Dilation Problems", *Journal of Engineering Mechanics*, ASCE, Vol.114, No.1, pp.181-187.

Pile Segment Tests-Sabine Pass. (1986) : "Some Aspects of the Fundamental Behavior of Axially Loaded Piles in Clay Soils", *ETC Report No.85-007*, Earth Technology Corp., Houston, Texas.

POULOS, H.G. and DAVIS, E.H. (1980) : *Pile Foundation Analysis and Design*, John Wiley and Sons, New York.

TROCHANIS, A.M., BIELAK, J. and CHRISTIANO, P. (1988) : "A Three-Dimensional Nonlinear Study of Piles Leading to the Development of a Simplified Model", *Technical Report of Research Sponsored by NSF Grant ECE-86/1060 Carnegie Mellon University*, Washington, D.C.

WATHUGALA, G.W. (1990) : "Finite Element Dynamic Analysis of Nonlinear Porous Media with Applications to Piles in Saturated Clays", *Ph.D. Dissertation*, Dept. of Civil Eng. and Eng. Mechanics, Univ. of Arizona, Tucson, Arizona.

WATHUGALA, G.W. and Desai, C.S. (1993) : "Constitutive Model for Cyclic Behavior of Clays. I: Theory", *Journal of Geotechnical Engineering*, ASCE, Vol.119, No.4, pp.714-729.

WOLF, J.P. (1985) : *Dynamic Soil-Structure-Interaction*, Prentice-Hall, Inc., Englewood Cliffs, New Jersey.

WU, G. and FINN, W.D.L. (1997) : "Dynamic Nonlinear Analysis of Pile Foundations using Finite Element Method in the Time Domain", *Canadian Geotechnical Journal*, Vol.34, pp.44-52.

ZIENKIEWICZ, O.C. (1977) : *The Finite Element Method*, 3rd Edition, McGraw-Hill Book Company, U.K.

Notations

a_0 = Dimensionless frequency $(= \omega * d/V_s)$

a_r = Dimensionless frequency $(= \omega * r_0/V_s)$

C = Global damping matrix

C_m = Material damping matrix

C_r = Radiation damping matrix

c_r = Damping coefficient for lateral direction

c_w = Damping coefficient for vertical directions

D = Damping ratio of soil;

d = Dimension of pile in cross-section (square);

E_p = Young's modulus for pile

E_s = Young's modulus for soil

F = Dimensionless yield surface for HiSS soil model

f = Frequency of excitation in Hz

G = Shear modulus for soil

h_1 = A material parameter in HiSS soil model

h_2 = A material parameter in HiSS soil model

i = imaginary unit = $\sqrt{-1}$

J_1 = First invariant of stress tensor

J_{2D} = Second invariant of deviatoric stress tensor

K = Global stiffness matrix

k = Real part of the dynamic stiffness

k' = Imaginary part of the dynamic stiffness

K_c = Complex dynamic stiffness for the soil-pile system

k_r^* = Complex stiffness coefficient in lateral direction

k_r = Stiffness coefficient (real part) in lateral direction

k_w^* = Complex stiffness coefficient in vertical direction

k_w = Stiffness coefficient (real part) in vertical direction

k_{st} = Static stiffness of the soil-pile system in horizontal direction

L = Length of the pile/ height of the soil stratum

M = Global mass matrix

P_0 = Amplitude of the force applied at pile head

p_a = Atmospheric pressure

P_F = Pseudostatic response influence coefficient vector

${}^tR$ = Nodal external force vector at time

r_0 = Distance from center of pile to the finite element boundary

S_1 = Dimensionless parameter for stiffness in lateral direction

S_2 = Dimensionless parameter for damping in lateral direction

S_{w1} = Dimensionless parameter for stiffness in vertical direction

S_{w2} = Dimensionless parameter for damping in vertical direction

t_1 = Time lag between force and displacement for inertial loading

${}^tU$ = Relative nodal displacement vector at time

${}^t\dot{U}$ = Relative nodal velocity vector at time

$^{t}\ddot{U}$ = Relative nodal acceleration vector at time

U_0 = Amplitude of input bed rock motion

U_c = Complex amplitude of displacement at the pile head

U_g = Amplitude of free field ground motion

U_p = Amplitude of pile head motion

$\ddot{V}_b$ = Bedrock acceleration at a particular time step

V_s = Shear wave velocity of the soil

Δt = Time step incremen

δ_0^* = Basic version of HiSS soil model, modified for clays

$d\varepsilon_{ij}^p$ = Incremental plastic strain tensor

α_{ps} = Hardening function in HiSS soil model

γ = A material parameter in HiSS soil model

η = A material parameter in HiSS, related to phase change poin

λ = Plasticity parameter (a constant of proportionality)

ν_p = Poisson's ratio of pile

ν_s = Poisson's ratio of soil

ρ_p = Mass density of pile

ρ_s = Mass density of soil

σ_{ij} = Stress tensor

ω = Circular frequency of excitation

ω_0 = Predominant circular frequency of loading

ξ_v = Volumetric plastic strain

θ = Phase lag in radians